



GC-MS Profiling and *In Silico* Studies to Identify Potential SARS-CoV-2 Nonstructural Protein Inhibitors from *Psidium guajava*

Ifeanyi Edozie Otuokere^{a,*}, Onyinye Uloma Akoh^a, Felix Chigozie Nwadire^a, Chinedum Ifeanyi Nwankwo^b, Joy Nwachukwu Egbucha^c, Chiemela Wisdom^a, Ogonna Augustine Okwudiri^b

^aDepartment of Chemistry, Michael Okpara University of Agriculture, Nigeria

^bDepartment of Biochemistry, Michael Okpara University of Agriculture, Nigeria

^cDepartment of Chemistry, University of Agriculture and Environmental Sciences, Nigeria

Abstract

The COVID-19 pandemic, caused by the SARS-CoV-2, has prompted international concern. The aim of this study is to identify SARS-CoV-2 nonstructural protein inhibitors-potentially bioactive phytochemicals from the traditional plant *Psidium guajava*. GC-MS analysis of *P. guajava* methanol leaves was investigated. *In silico* molecular docking, drug-likeness, toxicity, and prediction of the compounds' substance activity spectra (PASS) were evaluated. GC-MS analysis identified thirty (30) phytochemicals. According to molecular docking, all the phytochemicals have strong binding energies. The phytochemical beta bisabolene gave the best binding affinity of -5.0 kcal/mole. The detected compounds were all in accordance with Lipinski's Rule of Five (RO5). This showed that the identified *P. guajava* compounds would have lower attrition rates during clinical trials and thus have a better chance of being marketed. According to this research, a potential COVID-19 drug could be created using the newly identified phytochemicals of *P. guajava*.

DOI:10.46481/asr.2022.1.3.52

Keywords: Docking, GC-MS, Leaves, *P. guajava*, SARS-CoV-2

Article History :

Received: 18 August 2022

Received in revised form: 11 October 2022

Accepted for publication: 25 October 2022

Published: 29 December 2022

© 2022 The Author(s). Published by the Nigerian Society of Physical Sciences under the terms of the Creative Commons Attribution 4.0 International license. Further distribution of this work must maintain attribution to the author(s) and the published article's title, journal citation, and DOI.

Communicated by: Ayobami H. Labulo

*Corresponding author tel. no: +234 7065297631

Email address: ifeanyiotuokere@gmail.com (Ifeanyi Edozie Otuokere)

1. Introduction

Globally, the weekly number of COVID-19 cases has stabilized, with over 3.6 million cases recorded on 15 May, 2022, following the sustained decline observed since the end of March 2022. In comparison, over 9,000 fatalities were recorded during the same period; a 21% decrease from the previous week. This indicates that weekly fresh fatalities are continuing to decline. At the regional level, the number of new cases each week grew (+63%) in the Eastern Mediterranean Region, (+26%) in the Region of the Americas, (+14%) across the Western Pacific, and (+6%) in the African Region. All regions witnessed fewer deaths per week, with the exception of the African Region, which had a reported 48% increase in new deaths per week. Globally, more than 6 million fatalities and over 518 million confirmed cases had been documented as of May 15, 2022 [1].

Worldwide, medicinal plants and their bioactive components are utilized to treat a wide range of illnesses. According to reports, over 82% of people use medicinal plants or their bioactive substances to prevent, treat, or manage a variety of disorders [2]. Medicinal plants and their biologically active compounds have recently attracted the interest of many scientists and researchers because of their use in the development of new drugs or the identification of natural therapeutic components [3], as well as in the treatment of serious illnesses like cancer, diabetes, and hypertension [4]. *P. guajava* is one of the plants used in traditional medicine to treat a wide range of illnesses. Guava is the common name for *P. guajava* L. It is a tropical food shrub plant of the Myrtaceae family [5]. It is a 10 m tall plant that is widely available in many nations. The plant, *P. guajava*, a significant food crop, has a range of therapeutic benefits. It has a thin trunk with peeling, smooth, and uneven bark [5].

In ethnomedicine, *P. guajava*'s various parts, including the stem, bark, fruits, leaves, and roots are used to treat conditions like diarrhea, rheumatism, diabetes, laryngitis, malaria, cough, bacterial infections, and ulcers [5]. Many natives use decoctions, infusions, and/or boiled preparations of *P. guajava* topically or orally [6]. *P. guajava* leaves can be applied topically, while aqueous leaf extract can be taken internally by diabetics to lower their blood glucose levels [7]. *P. guajava* contains essential chemical components such as flavonoids, phenols, triterpenes, alkaloids, saponins, carotenoids, lectins, vitamins, carbohydrates, dietary fiber, fatty acids, glycosides. guaijaverin, quercetin, kaempferol, apigenin, catechin, chlorogenic acid, hyperin, gallic acid, epigallocatechin gallate. Phylloquinone and gallate are just a few of the many beneficial phenolic compounds found in the leaves [8]. Numerous studies have demonstrated the abundance of the following essential oils in the leaves of *P. guajava* [9]. These include b-caryophyllene, pinene, caryophyllene oxide, 1,8-cineole, and limonene [9]. In addition, pectin, protein, vitamins A and C, and minerals like iron, phosphorus, and calcium are all abundant in the fruit [10].

Molecular docking, an *in silico* method, is extremely beneficial since it lowers the cost of wet-lab research, saves animals, time, and resources, and properly guides medication selection and production. Molecular docking simulation's objective is to anticipate a ligand's binding affinity with a protein and the most stable complex; the lower or more negative the binding affinity, the better. Molecular docking simulation has simplified and verified *in vivo* and *in vitro* studies, as well as drug modeling and design for pharmaceutical researchers [11].

GC-MS analysis has been employed to uncover phytochemicals in numerous plants such as *Landolphia dulcis* [12], *Pausinystalia yohimbe* leaves [13], *Euphorbia hirta* leaves [14], *Combretum hispidum* root [15], *Buchholzia Coriacea* seed [16], *Combretum hispidum* leaves [17], *Justicia carnea* [18], *Chromolaena Odorata* [19], *Mimosa pudica* leaves [20] *Moringa oleifera* leaves [21], and *Allophylus africanus* stem bark [22]. The structural formula of bioactive chemicals found in *P. guajava* leaves has not been adequately characterized. There is minimal information on the characterization of *P. guajava* leaves by GC-MS and molecular docking studies of its bioactive phytochemicals. To bridge this gap, we have decided to identify *P. guajava* leaves using GC-MS analysis, perform molecular docking, drug-likeness, and prediction of activity spectra for substances on the identified compounds. The aim of this work is to use GC-MS and molecular docking to uncover possible SARS-CoV-2 inhibitors in *P. guajava* leaves.

2. Materials and Methods

2.1. Extraction

Leaves of *P. guajava* were harvested in Umudike, Abia, Nigeria on January, 2022. The plant was identified and given the herbarium number by the Taxonomy section of the Michael Okpara University of Agriculture, Umudike (MOUUAU) Forestry Department. After washing the leaves to remove grit, the leaves were weighed after four weeks

of air drying. It was macerated in methanol for 3 days, then decanted, filtered using Whatman No.1 filter paper, and concentrated with a rotary evaporator under lower pressure to get 8 g of extract.

2.2. GC-MS Analysis

The test was carried out on a 7890A GC-MS Triple Quad instrument (Agilent Technologies, Santa Clara, USA). An HP-5MS 30 m-250 mm (i.d.) fused-silica capillary column (Agilent J & W Scientific, Folsom, CA, USA) was chemically coupled with a 5% diphenyl and 95% dimethylpolysiloxane cross-linked stationary phase (0.25 mm film thickness). Exactly 1.5 μ L of the sample was injected at a particular linear diameter using helium as a carrier gas at 1.0 mL/min in split mode. Both the injector and supply were set to 250 °C. The oven's temperature was initially set at 40 °C and then gradually raised to 300 °C at a rate of 10 °C/min, for a total of 60 minutes. The temperature was set to 305 °C after the run and sustained for 1 minute. The mass spectrometer was operated in EI mode (70 eV). Data was collected in full scan mode with a scan time of 0.5 seconds from m/z 50 to 650. Agilent Mass Hunter Qualitative Analysis was used to evaluate the data (Version B.04.00). By comparing the average peak area of each component to the total areas, the relative percentage amounts of each component were computed.

2.3. Identification of phytochemical components

The constituents were identified using the retention index (RI, calculated using a homologous series of n-alkanes C8-C25 under identical experimental conditions), an MS library search (NIST 08MS Library Version 2.0 f; Thermo Fisher Scientific Austria), and data from the MS literature [23]. Without adding a correction factor, the relative concentrations of the various components were computed based on the GC peak area.

2.4. Preparation of SARS-CoV-2 viral protein and identified compounds

SARS-CoV-2 Nonstructural protein 1 (NSP1) (PDB ID: 7K3N) was obtained from the RCSB Protein Databank. Using the ArgusLab 4.0.1 software, water molecules and ions were removed, and polar hydrogens were added. The ACD/ChemDraw software was used to draw the structures of the identified compounds. Energy minimization was done using ArgusLab 4.0.1 software. ArgusLab 4.0.1 software was used to convert the structures of the identified compounds to PDB.

2.5. Molecular docking

For docking, AutoDock Vina, which was assembled in the PyRx Virtual Screening Tool, was used for docking [24]. PyRx is a computational therapeutic discovery virtual screening software with which libraries of compounds can be screened against prospective drug targets. The protein–ligand interaction profiler (PLIP) Server [25] was used to visualize the bond distances, types of interactions, and 3D images of all docked complexes.

2.6. Drug-likeness Prediction

Using Lipinski's RO5 [26], the drug-likeness parameters of the phytochemicals were assessed using the web server of Swiss ADME.

2.7. Toxicity Prediction in Silico Study

ProTox-II was used to predict toxicity and lethal dose (LD₅₀) for the identified chemicals.

2.8. In-Silico Prediction of Substance Activity Spectra (PASS) Study

The potential bioactivities of docked compounds were assessed using the internet program Prediction of Substance Activity Spectra (PASS).

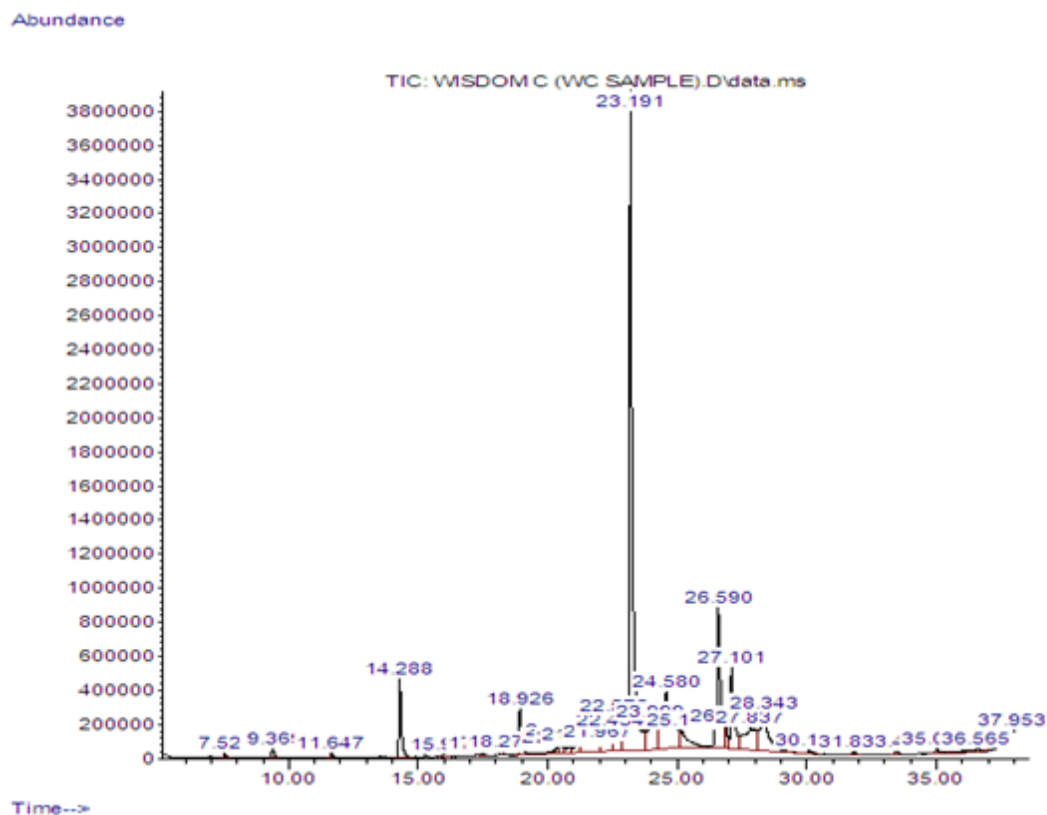


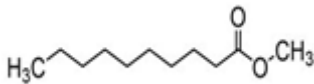
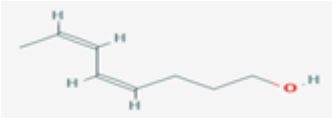
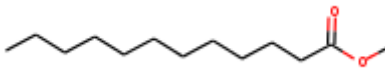
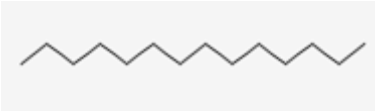
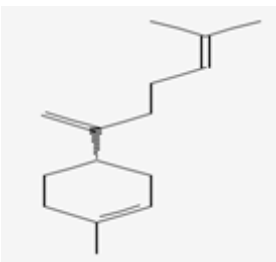
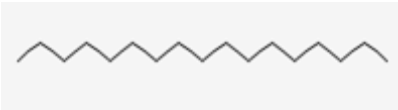
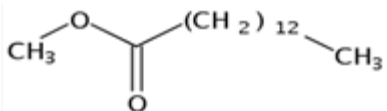

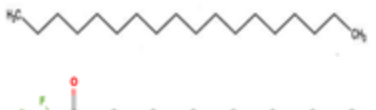


Figure 1. GC chromatogram of methanol extract from *P. guajava* leaves.

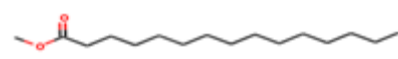
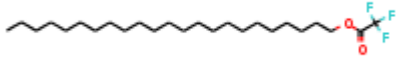
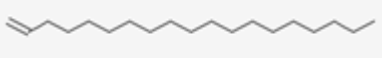



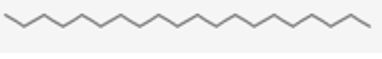
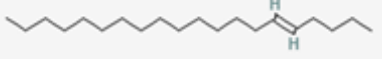
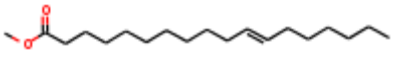
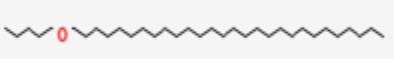
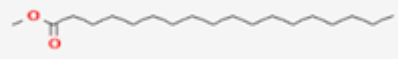

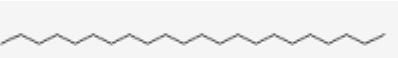

3. Results and Discussion


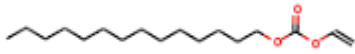
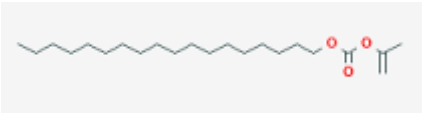
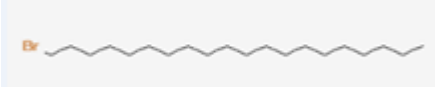
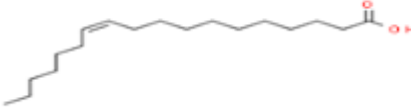
The GC–MS chromatogram of methanol extract from *P. guajava* leaves revealed a total of 30 peaks corresponding to bioactive compounds. Fig. 1 depicts the GC chromatogram. The compounds have been listed in Table 1. Table 2 shows the binding energies of phytochemicals from *P. guajava* leaves with SARS-CoV-2 (PDB ID: 7K3N). Figure 2 shows the 3D interaction of some identified compounds with SARS-CoV-2. A Drug-likeness prediction of the identified compounds in *P. guajava* leaf methanol extract is presented in Table 3. Toxicity prediction of the identified compounds in *P. guajava* leaf methanol extract by ProTox-II is shown in Table 4. Table 5 shows the predicted bioactivity of the identified compounds in *P. guajava* leaf methanol extract. Table 5 depicts the predicted bioactivity of the identified compounds in *P. guajava* leaf methanol extract.

Table 1: Phytochemicals Present in methanol extract of *P. guajava* leaves.

S/N	Retention time (mins)	Comp. (%)	Compound	Structure
1	7.523	0.17	Carvone	

2	9.369	0.41	Decanoic acid, methyl ester	
3	11.647	0.15	Cis-4,6-Octadienol	
4	14.288	3.39	Dodecanoic acid, methyl ester	 
5	15.979	0.14	Tetradecane	
6	17.455	0.16	Beta bisabolene	
7	18.273	0.12	Heptadecane	
8	18.926	2.32	Methyl tetradecanoate	
9	20.341	0.69	Carbonic acid, octadecyl 2,2,2-trichloroethyl ester	
10	20.471	0.77	Octadecane	
11	20.868	0.55	Pentafluoro propionic acid, pentadecyl ester	

12	21.102	0.93	Pentadecanoic acid, methyl ester	
13	21.967	2.13	Tricosyltrifluoroacetate	
14	22.454	2.61	I-Nonadecene	
15	22.575	4.02	Nonadecane	
16	23.191	36.45	Hexadecanoic acid, methyl ester	
17	23.999	4.60	Diethyl Phthalate	
18	24.580	10.28	Eicosane	
19	25.162	2.44	5-Eicosene, (E)	
20	26.590	9.73	11-Octadecenoic acid, methyl ester	
21	26.849	1.22	Octacosylpentyl ether	
22	27.101	5.76	Methyl stearate	
23	27.837	4.94	9,17-Octadecadienal, (Z)	
24	28.343	6.02	Docosane	
25	30.114	0.27	1-bromodocosane	

26	31.816	0.22	Carbonic acid, octadecyl vinyl ester	
27	33.453	0.21	Carbonic acid, tetradecyl vinyl ester	
28	35.024	0.26	Carbonic acid, octadecyl prop-1-en-2-yl ester	
29	36.565	0.46	1-Bromoeicosane	
30	37.953	-1.39	Cis-Vaccenic acid	

The 3D interaction of beta bisabolene with SARS-CoV-2 is shown in Figure 2a. Hydrophobic interactions were observed with protein residues VAL 11A, GLN 13A, VAL 14A, GLU 46A, GLU 48A, VAL 51A, and VAL 107A with bond distances of 3.99, 3.63, 3.66, 3.72, 3.76, 3.78, 3.76, and 3.68 Å. The 3D interaction of nonadecane with SARS-CoV-2 is shown in Figure 2b. Hydrophobic interactions were observed with protein residues VAL 11A, GLN 13A, VAL 14A, GLU 46A, GLU 48A, VAL 51A, and VAL 107A with bond distances of 3.99, 3.63, 3.66, 3.72, 3.76, 3.78, 3.76, and 3.68 Å. The 3D interaction of carbonic acid, octadecyl 2,2,2-trichloroethyl ester and SARS-CoV-2 is shown in Figure 2c. Hydrophobic interactions were observed with protein residues VAL 11A, GLN 13A, VAL 45A, GLU 46A, GLU 48A, VAL 51A, and VAL 107A with bond lengths of 3.87, 3.71, 3.88, 3.62, 3.72, and 3.58 Å. Hydrogen bonds were observed with protein residues ARG 15A, ARG 15A and GLN 54A with bond lengths of 2.69, 2.51 and 2.26 Å. The 3D interaction of carvone with SARS-CoV-2 is shown in Figure 2d. Hydrophobic interactions were observed with protein residues VAL 11A, GLN 13A, VAL 14A, ARG 15A, VAL 45A, GLU 46A, and VAL 51A with bond lengths of 3.71, 3.69, 3.58, 3.84, 3.98, 3.68, and 3.94 Å. The 3D interaction of carvone with SARS-CoV-2 is shown in Figure 2e. Hydrophobic interactions were observed with protein residues VAL 11A, GLN 13A, VAL 14A, VAL 45A, GLU 46A, GLU 48A and VAL 51A with bond lengths of 3.72, 3.86, 3.94, 3.68, 3.65, 3.70, 3.91, and 3.37 Å. Hydrogen bonds were observed with protein residues ARG 15A and ARG 15A with bond lengths of 2.32 and 2.27 Å. The 3D interaction of methyl stearate with SARS-CoV-2 is shown in Figure 2f. Hydrophobic interactions were observed with protein residues VAL 11A, GLN 13A, VAL 14A, VAL 14A, ARG 15A, VAL 45A, GLU 46A, GLU 48A, and GLU 48A with bond lengths of 3.78, 3.69, 3.63, 3.91, 3.59, 3.58, 3.59, 3.86, and 3.76 Å. The 3D interaction of pentafluoro propionic acid and pentadecyl ester with SARS-CoV-2 is shown in Figure 2g. Hydrophobic interactions were observed with protein residues GLN 13A, GLN 13A, VAL 14A, ARG 15A, GLU 46A, and VAL 107A with bond lengths of 3.49, 3.72, 3.38, 3.61, 3.78, and 3.86 Å. A hydrogen bond was observed with protein residue GLN 54A with a bond length of 2.01. A salt bridge was observed between the protein residue ARG 15A and the carboxylate group of the ligand with a bond distance of 3.61 Å. The 3D interaction of hexadecanoic acid and methyl ester with SARS-CoV-2 is shown in Figure 2h. Hydrophobic interactions were observed with protein residues VAL 11A, GLN 13A, VAL 14A, GLU 46A, GLU 48A, VAL 51A, and VAL 107A with bond distances of 3.78, 3.36, 3.70, 3.50, 3.95, 3.81, 3.50, and 3.52 Å. The 3D interaction of iodecanoic acid and methyl ester with SARS-CoV-2 is shown in Figure 2i. Hydrophobic interactions were observed with protein residues VAL 14A, VAL

Table 2. Binding energies of phytochemicals from *P. guajava* leaves with SARS-CoV-2 (PDB ID: 7K3N).

S/No	Compound	Binding affinity (Kcal/mol)
1	Carvone	-4.6
2	Decanoic acid, methyl ester	-3.8
3	Cis-4,6-Octadienol	-3.7
4	Dodecanoic acid, methyl ester	-4.0
5	Tetradecane	-3.5
6	Beta bisabolene	-5.0
7	Heptadecane	-3.5
8	Methyl tetradecanoate	-3.6
9	Carbonic acid, octadecyl 2,2,2-trichloroethyl ester	-3.9
10	Octadecane	-3.8
11	Pentafluoro propionic acid, pentadecyl ester	-4.5
12	Pentadecanoic acid, methyl ester	-3.8
13	Tricosyltrifluoroacetate	-4.1
14	I-Nonadecene	-3.6
15	Nonadecane	-4.3
16	Hexadecanoic acid, methyl ester	-3.9
17	Diethyl Phthalate	-4.6
18	Eicosane	-3.6
19	5-Eicosene, (E)	-3.6
20	11-Octadecenoic acid, methyl ester	-3.9
21	Octacosylpentyl ether	-3.5
22	Methyl stearate	-4.0
23	9,17-Octadecadienal, (Z)-	-4.1
24	Docosane	-3.7
25	1-Bromodocosane	-3.6
26	Carbonic acid, octadecyl vinyl ester	-3.8
27	Carbonic acid, tetradecyl vinyl ester	-4.1
28	Carbonic acid, octadecyl prop-1-en-2-yl ester	-4.2
29	1-Bromoeicosane Complex	-3.8
30	Cis-vaccenic acid	-4.1

45A, GLU 46A, GLU 48A, GLU 48A and VAL 51A with bond distances 3.91, 3.94, 3.92, 3.76, 3.92, and 3.67 Å. A hydrogen bond was observed with protein residue GLU 46A with a bond distance of 1.82 Å. The 3D interaction of carbonic acid and octadecyl prop-1-en-2-yl ester with SARS-CoV-2 is shown in Figure 2j. Hydrophobic interactions were observed with protein residues GLU 46A, VAL 47A, VAL 47A, LEU 52A, PHE 61A, and LEU 95A with bond distances 3.61, 3.69, 3.57, 3.87, 3.53, and 3.61 Å. A hydrogen bond was observed with protein residues LYS 63A and GLN 87A with bond distances of 2.27 and 2.57 Å.

The RO5 is a thumb rule for identifying whether a compound with a specific bioactivity has physical and chemical features that indicate it would be an orally active drug. All of the identified compounds meet the RO5 criteria. As a result, the identified *P. guajava* leaf methanol extract lead molecules will have reduced attrition rates throughout clinical trials, giving them a better chance of commercialization [26].

Toxicity predictions reveal that compounds 1, 5, 6, 7, 8, 9, and 10 may be harmful if consumed ($2000 < LD_{50} \leq 5000$ mg/kg). Compound 2 is lethal if consumed ($5 < LD_{50} \leq 50$ mg/kg). Compounds 3 and 4 are harmful if consumed ($300 < LD_{50} \leq 2000$ mg/kg).

Table 3. Drug-likeness prediction of the identified compounds in *P. guajava* leaf methanol extract.

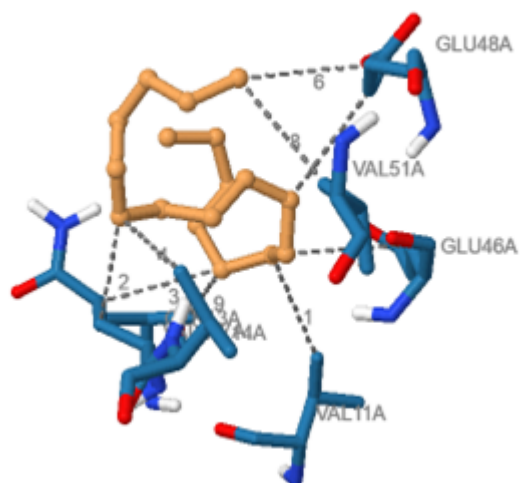
Compounds	Mol. weight (g/mol) ¹	HB Acceptor ²	HB Donor ³	Lipophilicity ⁴	Molar refractivity ⁵	Rule of five ⁶
Betabisabolene	204.35	0	0	3.67	70.68	1
Nonadecane	268.52	0	0	5.46	93.45	1
(Carbonic acid, octadecyl 2,2,2-trichloroethyl ester	445.89	3	0	6.19	120.25	1
carvone	150.22	1	0	2.27	47.32	0
(Carbonic acid, tetradecyl vinyl ester	284.43	3	0	4.81	86.12	0
methyl stearate	298.50	2	0	4.81	94.73	1
(Pentafluoropropionic acid, pentadecyl ester	374.43	7	0	4.88	90.26	1
Hexadecanoic acid, methyl ester	270.45	2	0	4.41	85.12	1
Dodecanoic acid, methyl ester	214.34	2	0	3.48	65.89	0
Carbonic acid, octadecyl prop-1-en-2-yl ester	354.57	3	0	5.90	110.15	1

¹ Molecular weight (acceptable range: <500). ² HB, Hydrogen bond acceptor (acceptable range: ≤ 10). ³ HB, Hydrogen bond donor (acceptable range: ≤ 5). ⁴ Lipophilicity (Log Po/w, acceptable bounds <5). ⁵ Molar refractivity, acceptable bounds 40 – 130. ⁶ RO5: Number of RO5 violations ideal range: 0–4.

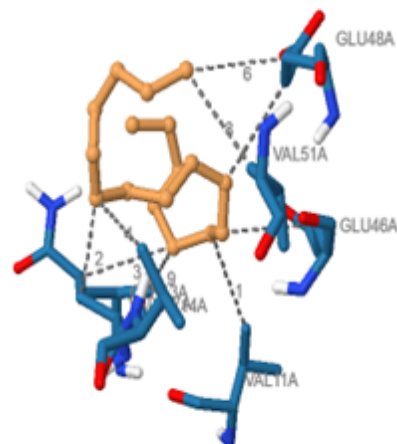
Table 4. Toxicity prediction of the identified compounds in *P. guajava* leaf methanol extract by ProTox-II.

S/No	Compound	Predicted LD ₅₀ (mg/kg)	Predicted Toxicity Class
1	Beta bisabolene	4400	5
2	Nonadecane	750	3
3	Carbonic acid, octadecyl 2,2,2-trichloroethyl ester	1190	4
4	Carvone	1640	4
5	(Carbonic acid, tetradecyl vinyl ester	4400	5
6	methyl stearate	5000	5
7	Pentafluoropropionic acid, pentadecyl ester	5000	5
8	Hexadecanoic acid, methyl ester	5000	5
9	Dodecanoic acid, methyl ester	5000	5
10	(Carbonic acid, octadecyl prop-1-en-2-yl ester	5000	5

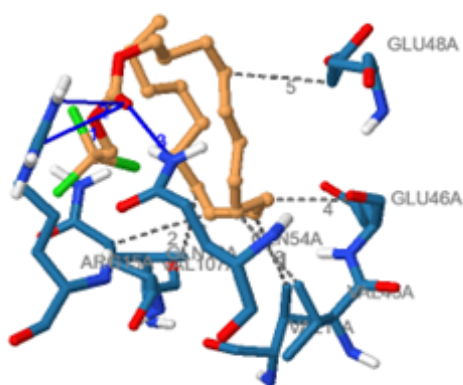
^a ProTox (http://tox.charite.de/protox_II, accessed on 7 March, 2022) Class 1: deadly if consumed ($LD_{50} \leq 5$); Class 2: deadly if consumed ($5 < LD_{50} \leq 50$); Class 3: lethal if consumed ($50 < LD_{50} \leq 300$); Class 4: harmful if consumed ($300 < LD_{50} \leq 2000$); Class 5: maybe harmful if consumed ($2000 < LD_{50} \leq 5000$); Class 6: non-lethal ($LD_{50} > 5000$).



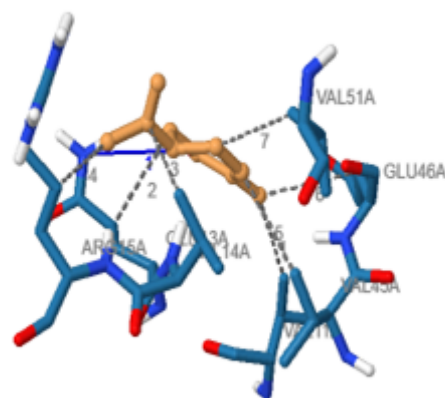
(a)



(b)



(c)

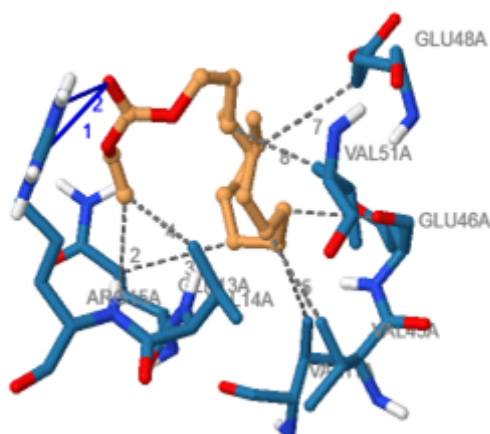


(d)

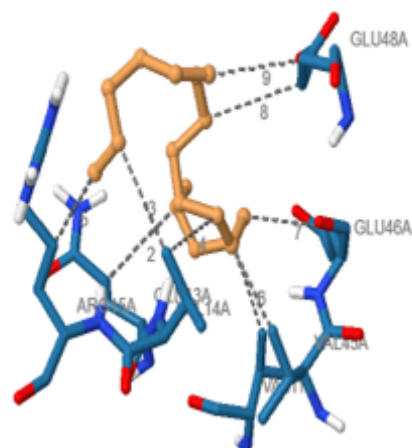
Table 5. Predicted bioactivity of the identified compounds in *P. guajava* leaf methanol extract.

Compounds	Pa	Pi	Biological activity
Beta bisabolene	0.908	0.001	Retinol dehydrogenase inhibitor
Nonadecane	0.954	0.002	Sugar-phosphatase inhibitor
Carbonic acid, octadecyl 2,2,2-trichloroethyl ester	0.978	0.001	Alkanal monooxygenase (FMN-linked) inhibitor
Methyl stearate	0.962	0.002	Saccharopepsin inhibitor
Pentafluoropropionic acid,	0.960	0.002	Eye irritation, inactive
Hexadecanoic acid, methyl ester	0.962	0.002	Saccharopepsin inhibitor
Dodecanoic acid, methyl ester	0.962	0.002	Saccharopepsin inhibitor
Carbonic acid, octadecyl prop-1-en-2-yl ester	0.945	0.001	Alkanal monooxygenase (FMN-linked) inhibitor
Carvone	0.968	0.002	CYP2B1 substrate
Carbonic acid, tetradecyl vinyl ester	0.978	0.001	Alkanal monooxygenase (FMN-linked) inhibitor

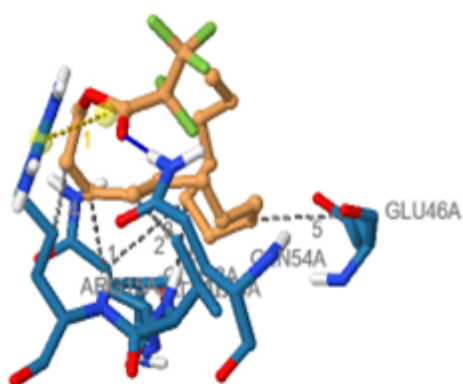
^aPa = Possibility of activity; ^bPi = Possibility of inactivity.



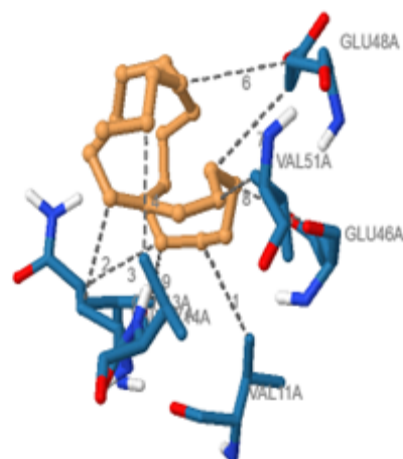
(e)



(f)



(g)



(h)

The docked compounds' potential biological activities were assessed using PASS, an online Structure-based bioactivity prediction tool (Table 5). The PASS analysis determined the probable targets and biological activities of each compound. We looked at the biological activity for each molecule based on $P_a > P_i$ and $P_a > 0.7$ values. The results demonstrated a variety of biological activities with $P_a > 0.908$, showing that the identified compounds in the leaves of *P. guajava* have a broad potential aside the *in silico* inhibition of SARS-CoV-2. It was discovered that there were numerous unknown pharmacological actions in each case in the PASS spectrum of the chosen phytoconstituent. PASS-predicted activities provided the basis for assessing the untapped potential of *P. guajava* leaves.

4. Conclusion

The leaves of *P. guajava* were found to be a rich source of bioactive phytochemicals in the GC-MS investigation. Docking experiments indicated high affinity for the NSP1 SARS-CoV-2. Drug-likeness indicated that the phytochemicals conformed to RO5. The PASS analysis approach predicted many bioactive actions of the phytochemicals

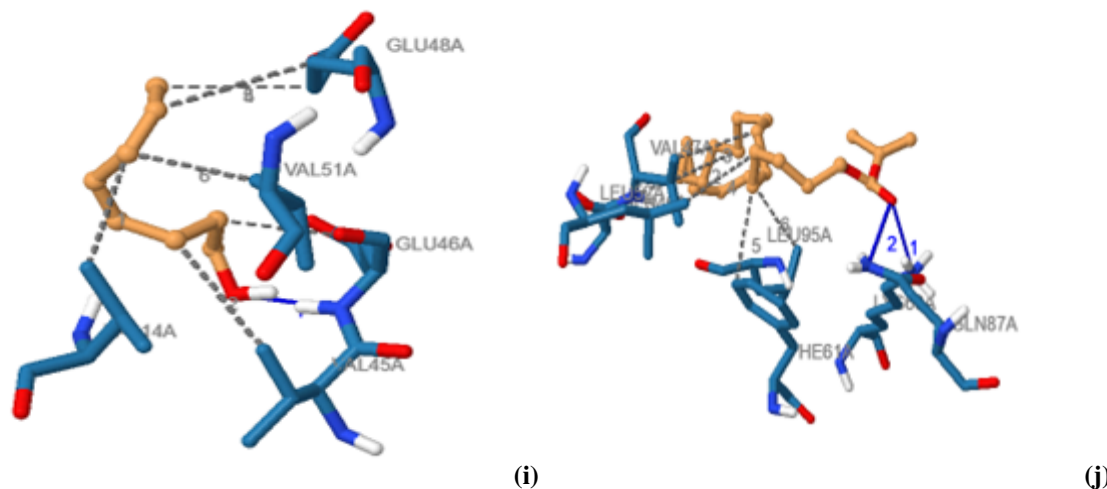


Figure 2. Three-dimensional interactions of some identified compounds with SARS-CoV-2. (a) beta bisabolene (b) nonadecane (c) carbonic acid, octadecyl 2,2,2-trichloroethyl ester (d) carvone (e) carbonic acid, tetradecyl vinyl ester (f) methyl stearate (g) pentafluoro propionic acid, pentadecyl ester (h) hexadecanoic acid, methyl ester (i) dodecanoic acid, methyl ester (j) carbonic acid, octadecyl prop-1-en-2-yl ester.

studied. The molecular docking studies suggested that *P. guajava* leaves could be a viable natural antiviral option for SARS-CoV-2. This research can be extended by isolating pure compounds responsible for the bioactivity discovered, as well as assessing their toxicity profile and long-term safety.

Acknowledgements

We are grateful to the Michael Okpara University of Agriculture, Umudike for allowing us to use the facilities in Chemistry laboratory.

References

- [1] World Health Organization, “COVID-19 Weekly Epidemiological Update”, World Health. Organization **92** (2022) 33.
- [2] B. Pant, “Application of Plant Cell and Tissue Culture for the Production of Phytochemicals in Medicinal Plants”, *Advances in Experimental Medicine and Biology* **808** (2014) 25.
- [3] M. Pia, A. Stefanucci, A. Della, G. Scioli, A. Cichelli & A. Mollica, “ An overview on plants cannabinoids endorsed with cardiovascular effects”, *Biomedicine Pharmacotherapy* **142** (2021) 111963.
- [4] A. Sofowora, E. Ogunbodede & A. Onayade, “The role and place of medicinal plants in the strategies for disease”, *African Journal of Traditional and Complementary Alternative Medicine* **10** (2013) 210.
- [5] K. Ravi & P. Divyashree, “*Psidium guajava*: A review on its potential as an adjunct in treating periodontal disease”, *Pharmacognosy Reviews* **8** (2016) 96.
- [6] E. Díaz-de-cerio & A. M. Gómez-caravaca, “Determination of guava (*Psidium guajava* L .) leaf phenolic compounds using HPLC-DAD-QTOF-MS”, *Journal of Functional Foods* **22** (2016) 376
- [7] R. M. P. Gutiérrez, S. Mitchell & R.V. Solis, “*Psidium guajava* : A review of its traditional uses , phytochemistry and pharmacology”, *Journal of Ethnopharmacology* **117** (2008) 7.
- [8] M. Kumar et al, “Guava (*Psidium guajava* L .) Leaves : Nutritional Composition”, *Foods* **10** (2021) 3.
- [9] J. Al-sabahi, A. Weli, A. Al-kaabi, J. Al-sabahi, S. Said & M. Amzad, “Chemical composition and biological activities of the essential oils of *Psidium guajava* leaf ;” *Journal of King Saud University - Science* **31**(2019) 993.
- [10] S. Naseer, S. Hussain, N. Naeem, M. Pervaiz & M. Rahman, “The phytochemistry and medicinal value of *Psidium guajava* (guava)”, *Clinical Phytoscience* **4** (2018) 32.
- [11] A. Fitriah , K. Holil, U. Syarifah & U.D.H Fitriyah, “In silico approach for revealing the anti- breast cancer and estrogen receptor alpha inhibitory activity of *Artocarpus altalis*”, *AIP Conference Proceedings* **070003** (2018) 1.
- [12] I. E. Otuokere, F. J. Amaku, K. K. Igwe & C. A. Bosah, “Characterization of *Landolphia dulcis* Ethanol Extract by Gas Chromatography - Mass Spectrometry Analysis,” *International Journal on Advances in Engineering Technology and Science* **2** (2016)13.
- [13] K. K. Igwe, A. J. Madubuike, C. Ikenga, I. E. Otuokere & F. J. Amaku, “Studies of the medicinal plant *Pausinystalia yohimbe* ethanol leaf extract phytocomponents by GCMS analysis”, *International Journal of scientific Research and Management* **4** (2016) 4116.

- [14] K. K. Igwe, A. J. Madubuike, S. C. Akomas, I. E. Otuokere & C.S. Ukwueze, “Studies of the medicinal plant *Euphorbia hirta* methanol leaf extract phytocomponents by GCMS analysis”, *International Journal of Scientific and Technical Research in Engineering* **1** (2016) 9.
- [15] O. V Ikpeazu, I. E. Otuokere & K. K. Igwe, “Gas Chromatography – Mass Spectrometric Analysis of Bioactive Compounds Present in Ethanol Extract of *Combretum hispidum* (Laws) (Combretaceae) Root”, *Communications in Physical Sciences* **5** (2020) 325.
- [16] I. E. Otuokere & K. K. Igwe, “Preliminary Studies on the Secondary Metabolites of *Buchholzia Coriacea* (Wonderful Kola) Seed Ethanol Extract by GC-MS Analysis”, *International Journal of Research in Engineering and Applied Sciences* **7** (2017) 17.
- [17] O. V Ikpeazu, I. E. Otuokere & K. K. Igwe, “GC – MS Analysis of Bioactive Compounds Present in Ethanol Extract of *Combretum hispidum* (Laws) (Combretaceae) Leaves”, *International Journal of Trend in Scientific Research and Development* **4** (2020) 307.
- [18] I. E. Otuokere, A. J. Amaku, K. K. Igwe & G. C. Chinedum, “Medicinal Studies on the Phytochemical Constituents of *Justicia carnea* by GC-MS Analysis”, *American Journal of Food Science and Health* **2** (2016) 71.
- [19] I. E. Otuokere, D. O. Okorie, K. K. Igwe & U. J. Matthew, “Gas Chromatography-Mass Spectrometry Determination of Bioactive Phyto-compounds in *Chromolaena Odorata* Leaf Extract”, *International Journal on Advances in Engineering Technology and Science* **2** (2016) 7.
- [20] A. A. Ahuchaogu, G. I. Ogbuehi, P. O. Ukaogo & I. E. Otuokere, “Gas Chromatography Mass Spectrometry and Fourier transform Infrared Spectroscopy analysis of methanolic extract of *Mimosa pudica* L. leaves”, *Journal of Drugs and Pharmaceutical Science* **4** (2020) 1.
- [21] K. K. Igwe, P. O. Nwankwo, I. E. Otuokere, S. N. Ijioma & F. J. Amaku, “GCMS analysis of Phytocomponents in the Methanolic Extract of *Moringa oleifera* Leaf,” *Journal of Research in Pharmaceutical Science* **2** (2015) 1.
- [22] R.P. Adams, *Identification of Essential Oil Components by Gas Chromatography/Mass Spectroscopy*, Allured Publishing, Carol Stream, Ill, USA (2007) 15.
- [23] S. Dallakyan & A. J. Olson, *Small-Molecule Library Screening by Docking with PyRx*,” *Methods in Molecular Biology*, Springer Science+Business Media, New York (2015) 243.
- [24] M. F. Adasme, K.L. Linnemann, S. N. Bolz, F. Kaiser, S. Salentin, V. J. Haupt & M. Schroeder, “PLIP 2021 : expanding the scope of the protein – ligand interaction profiler to DNA and RNA”, *Nucleic Acids Research* **49** (2021) 530.
- [25] C. A. Lipinski, F. Lombardo, B. W. Dominy & P. J. Feeney, “Experimental and computational approaches to estimate solubility and permeability in drug discovery and development settings”, *Advanced Drug Delivery Reviews* **46** (2001) 3.
- [26] R.K. Goel, D. Singh, A. Lagunin & V. Poroikov, “PASS-assisted exploration of new therapeutic potential of natural products,” *Medicinal Chemistry Research* **20** (2010) 1509.